



Alterations in the gut microbiota and its metabolic profile of PM_{2.5} exposure-induced thyroid dysfunction rats



Xinwen Dong^{a,*}, Sanqiao Yao^a, Lvfei Deng^a, Haibin Li^a, Fengquan Zhang^c, Jie Xu^c, Zhichun Li^a, Li Zhang^b, Jing Jiang^c, Weidong Wu^{a,*}

^a Department of Environmental and Occupational Health, School of Public Health, Xinxiang Medical University, Xinxiang, Henan Province 453003, China

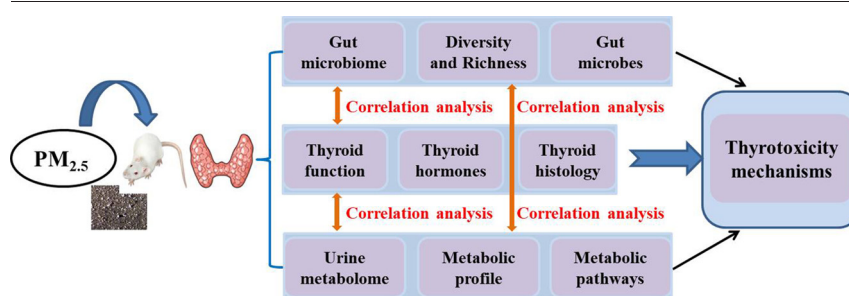
^b Center for Bioinformatics and Statistical Health Research, School of Public Health, Xinxiang Medical University, Xinxiang, Henan Province 453003, China

^c Experimental Teaching Center of Public Health and Preventive Medicine, School of Public Health, Xinxiang Medical University, Xinxiang, Henan Province 453003, China

HIGHLIGHTS

- 16S rRNA sequencing and LC-MS metabolomics were used to study the impact of PM_{2.5} on male rats' thyroid.
- PM_{2.5} exposure altered gut microbiome and its key metabolites related to thyroid function.
- PM_{2.5} exposure disturbed vital metabolic pathways related to thyroid thyrotoxicity.
- The gut-thyroid axis could be a new mechanism for PM_{2.5}-induced thyrotoxicity.

GRAPHICAL ABSTRACT



ARTICLE INFO

Editor: Jianmin Chen

Keywords:

PM_{2.5}
Thyrotoxicity
Microbiome
Metabonomics
Gut-thyroid axis
Metabolites

ABSTRACT

Fine particulate matter (PM_{2.5}) has drawn more and more interest due to its adverse effects on health. Thyroid has been demonstrated to be the key organ impacted by PM_{2.5}. However, the mechanisms for PM_{2.5} exposure-induced thyrotoxicity remain unclear. To explore the mechanisms, a rat thyroid injury model was established by exposing rats to PM_{2.5} via passive pulmonary inhalation. Thyroid hormones and thyroid function proteins were detected. The thyroid function affected by PM_{2.5} exposure was investigated via metabolomics analysis using liquid chromatography-mass spectrometry and 16S rRNA gene sequencing. Results showed that PM_{2.5} exposure induced remarkable alterations in gut microbiome evenness, richness, and composition. Metabolomics profiling revealed that the urine metabolites levels were changed by PM_{2.5} exposure. The altered gut microbiota and urine metabolites showed significant correlations with thyroid function indicators (total T3, total T4 and thyrotropin hormone, etc.). These metabolites were involved in metabolic pathways including thyroid hormone synthesis, metabolisms of tryptophan, D-Glutamine and D-glutamate, histidine, glutathione, etc. The altered gut microbiota showed significant correlations with urine metabolites (glutathione, citric acid, D-Glutamic acid, kynurenic acid and 5-Aminopentanoic acid, etc.). For example, the taurocholic acid levels positively correlated with the relative abundance of several genera including *Elusimicrobium* ($r = 0.9741, p = 0.000000$), *Muribaculum* ($r = 0.9886, p = 0.000000$), *Candidatus Obscuribacter* ($r = 0.8423, p = 0.000585$), *Eubacterium* ($r = 0.9237, p = 0.000017$), and *Parabacteroides* ($r = 0.8813, p = 0.000150$), while it negatively correlated with the relative abundance of *Prevotella* ($r = -0.8070, p = 0.001509$). PM_{2.5} exposure-induced thyrotoxicity led to remarkable alterations both in gut microbiome composition and some metabolites involved in metabolic pathways. The altered intestinal flora and metabolites can in turn influence thyroid function in rats. These findings may provide novel insights regarding perturbations of the gut-thyroid axis as a new mechanism for PM_{2.5} exposure-induced thyrotoxicity.

* Corresponding authors.

E-mail addresses: dongxinwen118@yeah.net (X. Dong), wduwu2013@126.com (W. Wu).

1. Introduction

The incidence of thyroid cancer has exhibited an increasing trend during the last few decades (Li et al., 2021b; Wirth et al., 2021). Air pollution is a potential risk factor for thyroid cancer, but the effect and mechanism remain unclear. PM_{2.5}, as a key environmental pollutant, influences human health worldwide, and the main route of PM_{2.5} exposure is contamination of atmosphere by air sources of fine particulate matter. Substantial diseases including liver, lung, bladder, and skin cancers, cardiovascular disorders, and diabetes (Lui et al., 2019), as well as metabolic and thyroid conditions, and male/female fertility (Colao et al., 2016) have been correlated with PM_{2.5} exposure. More recently, animal and human studies showed that there is a correlation between increased thyroid disease and PM_{2.5} exposure (Dong et al., 2021a; Irizar et al., 2021; Zeng et al., 2020). However, the specific pathophysiological mechanism of PM_{2.5}-induced thyroid injury remains unclear.

Multiple epidemiological studies showed that PM_{2.5} pollution was significantly related to hypothyroidism (CH) (Pan et al., 2019; Shang et al., 2019). Moreover, the influence of air pollution on FT4 levels of cord blood was mediated at least partially by placental iodine load (Neven et al., 2021). Second trimester prenatal PM_{2.5} exposure might interfere with maternal thyroid hormone (TH) levels (Zhao et al., 2019). Study found that PM_{2.5} exposure could cause hypothalamic inflammation and regulate the hypothalamic-pituitary axis (Xu et al., 2016). In our previous study, we found that PM_{2.5} exposure could hinder the biosynthesis and transport of thyroid hormones, alter the levels of thyroid hormone receptors, induce oxidative stress and inflammation, and eventually activate the hypothalamic-pituitary-thyroid (HPT) axis (Dong et al., 2021a). It may also activate the paraventricular nucleus of the hypothalamus, thereby activating the sympathetic nervous system and stress signaling, in turn activating the HPT axis. Serum concentrations of FT4 and TSH in older, overweight or obese adults were correlated with exposure to these air pollutants (Kim et al., 2020). Other studies showed that PM_{2.5} was related to thyroid (dys)function in pregnant women, and there was a dose-response relationship between TSH and PM_{2.5}, however, the underlying mechanisms remain unclear (Ilias et al., 2020). A cohort study showed that the newborn thyroid functions were correlated with prenatal PM exposure, especially during early pregnancy and midpregnancy (Howe et al., 2018). As a step in the biosynthesis of thyroid hormones, iodide oxidation was very sensitive to oxidative stress activation. The impaired iodide uptake and organification led to disturbed functions of thyroid cells (Nadolnik et al., 2008). Moreover, our previous study indicated that PM_{2.5} could affect the rats' thyroid function via altering the expression of thyroid stimulating hormone receptor (TSHR), sodium iodide symporter (NIS), thyroid-stimulating hormone beta (TSHβ), thyrotropin releasing hormone receptor (TRHR), thyroglobulin (TG), thyroid peroxidase (TPO), thyroid synthesis related transcription factor (PAX8, TTF-1, TTF-2) and liver transthyroxine (TTR). More recently, an ecological study showed that some air pollutants may increase incidence and mortality of thyroid cancer in men (Giannoula et al., 2020), suggesting that PM_{2.5} exposure is correlated with impaired thyroid function, which may result from oxidative stress and inflammation. Despite the aforementioned findings, the mechanism of PM_{2.5} exposure on the thyroid disease has not been fully elucidated. Treatments for thyroid disease are limited; therefore, studies on the pathogenic processes of thyroid injury led by PM_{2.5} exposure are required.

The gut microbiome plays critical roles in host metabolism modulation (Holmes et al., 2011). The gut microbiome composition can be influenced by diet, environment, antibiotics, and bacterial/viral infection. Therefore, toxic environmental chemicals induced alteration of gut microbiome might be the mechanism underlying the effects of environmental agents on human health. Recent studies found alterations of gut microbiome composition in thyroid nodules, thyroid cancer, Graves' disease and Hashimoto's thyroiditis (Zhang et al., 2019). The gut microbiome can influence health of whole body via gut-thyroid axis (Lerner et al., 2017). Numerous studies showed that alterations of gut microbiome and its impact on physiological and metabolic processes significantly affect progression of

thyroid diseases in humans (Li et al., 2021a; Moshkelgosha et al., 2018; Virili et al., 2021; Zhang et al., 2019). PM_{2.5} has a high toxicity, therefore the potential effects of PM_{2.5} exposure on gut microbiome as well as thyroid dysfunction need extensive study. Several studies reported associations between gut microbiome and environmental chemicals such as polychlorinated biphenyls, mercury and arsenic (Lin et al., 2021; Wahlang et al., 2021; Wang et al., 2021). Mass spectrometry-based analysis of metabolomics can provide more information than 16S rRNA gene sequencing on relationship between PM_{2.5} exposure and microbiome as well as thyrotoxicity, and therefore is widely applied in study of environmental pollutants (Chu et al., 2021). Metabolomic profiling can be used to unravel metabolic pathways underlying a disease (Cui et al., 2019). Alterations in metabolites induced by some pollutants have been found to be correlated with thyroid function (TT3, TT4, FT3, FT4 and TSH) (Villanger et al., 2020). Xu et al. reported significant alterations in mouse serum metabolome induced by PM_{2.5} exposure (Xu et al., 2019).

At present, the relationship between PM_{2.5} exposure-induced thyrotoxicity, gut microbiome, and its metabolic profile has not yet been elucidated. This study, for the first time, investigated the effect of PM_{2.5} exposure on thyroid function, gut microbiome and its metabolic profile in rats using an integrated approach combining 16S rRNA gene sequencing and liquid chromatography-mass spectrometry (LC-MS) metabolomics to determine whether bacterial genera and specific metabolites are associated with PM_{2.5} exposure-induced thyrotoxicity.

2. Materials and methods

2.1. Preparation of PM_{2.5}

PM_{2.5} was obtained using a large flow PM_{2.5} particulate sampling device (TE-6070 American TISCH) located at Xinxiang city, which is contaminated mainly by coal dust and industrial pollution, especially from November to January of the next year. Sampling time, the most polluted time in winter. The data were obtained using a PM_{2.5} concentration monitoring system (1405-F TEOMTM PM_{2.5} Monitor [EPA equivalent method: EQPM-0609-181]). The PM_{2.5} powder was dissolved in phosphate-buffered saline (PBS) at different concentrations.

2.2. Animals and PM_{2.5} exposure

SPF male Sprague-Dawley rats (60 ± 20 g) were purchased from SPF (Beijing) Biotechnology Co., Ltd. (License key: SCXK (Jing) 2019-0010), housed regularly for 5 days (d), and then randomly divided into four groups (10 rats/group): control group (C, 0 mg/kg), medium PM_{2.5}-dosed group (M, 10 mg/kg), high PM_{2.5}-dosed group (H, 20 mg/kg), and recovery PM_{2.5}-dosed group (R, 20 mg/kg, dosed for 35 d and no treatment for 14 d). This dosing design was selected according to previous published epidemiological (Chen et al., 2017) and animal studies (Zhang et al., 2017). PM_{2.5} was dissolved in saline solution according to the above concentrations. All rats were dosed with PM_{2.5} twice for 49 days daily via passive pulmonary inhalation (Jin et al., 2016). This study was approved by the Institute of Zoology Animal and Medical Ethics Committee of Xinxiang Medical University, and complied with international standards (NIH publications No 80-23 revised 1996).

2.3. Sample collection

The rats were anesthetized on day 49 using 10% sodium pentobarbital, and blood was collected via abdominal aorta. The serum was isolated and utilized for test of thyroid hormone and iodine levels. The stool was snap-frozen for 16S rRNA gene sequencing; the urine was collected one day before terminal for analysis of non-targeted metabolomics. These two omics experiments were conducted on control and 20 mg/kg PM_{2.5} groups. The thyroids and livers were collected from partial animals for the immunohistochemistry and western blot analyses. The thyroids collected from the rest

rats ($n = 4$) were subjected to hematoxylin and eosin (H&E) staining and microscopic examination.

2.4. Measurement of thyroid hormones and urine iodine levels

The levels thyrotropin hormone (TSH), total T4 (TT4), total T3 (TT3), and urine iodine (UI) were analyzed using ELISA kits by following the manufactures' instructions (Shanghai Future Industrial Co. Ltd., China).

2.5. Immunohistochemical staining and western blot analyses of thyroid function-related proteins

The paraffin sections of fixed thyroids and livers were incubated with NIS, TTF-1, TPO, TG, PAX8 and TTR antibodies at 4 °C overnight (Table S1), and then incubated with secondary antibodies at room temperature for 15 min, followed by a 15-min incubation with peroxidase-conjugated streptavidin, a 10-min incubation with diaminobenzidine (DAB) and a 5-min incubation with hematoxylin. The areal density index was applied to analyze the IHC results: Areal density = IOD/AREA. IHC micrographs were taken and analyzed using Image Pro-Plus 6.0 software (Media Cybernetics, Inc., Rockville, MD, USA).

Rat pituitary, hypothalamus, thyroid, and liver were homogenized, and proteins were separated with sodium dodecyl-sulfate polyacrylamide gel electrophoresis, and then transferred to PVDF membranes. After blockage with 5% bovine serum albumin, the membranes were incubated with primary antibodies (TRHR, TSH β and TTR) at 4 °C overnight, followed by in-cubation with HRP-conjugated secondary antibody (dilution 1:3000) at 37 °C for 1 h. After color development using an ECL kit, the films were scanned (V300, EPSON), and the optical densities of target bands were examined using gray level analysis software (AlphaEase FC, Alpha Innotech).

2.6. 16S rRNA gene sequencing for the gut microbiome

To explore the diversity and composition of fecal microbial community, high-throughput sequencing of fecal bacterial 16S rRNA genes was performed on an Illumina MiSeq platform (Majorbio, Inc., Shanghai, China) as described previously (Li et al., 2020). The CTAB/SDS method was used to extract total genomic DNA from samples in high PM_{2.5}-dosed and control groups, and the DNA concentration and purity were detected by NanoDrop 2000 spectrophotometer (Thermo Fisher, USA). The V4 region of the 16S rRNA gene was amplified using specific primers with the barcode (515F:

and 806R: GGACTACHVGGGTWTCTAAT). The PCR Master Mix (New England Biolabs, USA), forward and reverse primers, and the template DNA were prepared for the PCR reaction system, and then the amplification was conducted. The quality filtering about raw tags was performed according to the QIIME (Version 1.9.1). The $\geq 97\%$ similarity about sequences was belonged to the same operational taxonomic units (OTUs). The QIIME (Version 1.9.1) was used to calculate the alpha and beta diversities. The following indexes, including Simpson, Shan-non, Chao1, and ACE were used to evaluate the alpha diversity. Beta diversity analysis was used to evaluate differences of samples in species complexity, Beta diversity on weighted UniFrac was calculated using QIIME (Version 1.9.1). The separation of samples between the two groups was visualized by the principle coordinates analysis (PCoA). Metastats (<http://metastats.ccb.umd.edu/>) software was applied to conduct *t*-test on species richness between groups (White et al., 2009).

2.7. LC-MS based urine metabolomics and multivariate statistical analysis

The urine supernatant (200 μ L) of rats' urine in high PM_{2.5}-dosed and control groups was subjected to liquid chromatography-mass spectrometry (LC-MS) analysis as described previously (Dong et al., 2021b). The Ultra performance liquid chromatography (UPLC) software (Waters ACQUITY UPLC HSS T3 C18, USA) was used to quantify the metabolite concentrations. The LC-MS data was analyzed by a supervised orthogonal partial least-squares discriminant analysis (OPLS-DA) clustering method. Variable Importance in Projection (VIP) derived from the OPLS-DA analysis was used to screen a variable, and a VIP value ≥ 1 and $P \leq 0.05$ is marked as a discriminating metabolite in this study. Biological pathway analysis was performed based on LC-MS data using MetaboAnalyst 4.0. The impact value threshold calculated for pathway identification was set at 0.1.

2.8. Exploration and validation of the biological functions of the gut microbiome

The impact of PM_{2.5} exposure on the gut microbiome and its metabolic profiles were examined as described previously (Wu et al., 2021). Briefly, the gut microbiome changes induced by PM_{2.5} exposure were revealed by the QIIME and Metastats software packages. The XCMS software was used to analyze the metabolites, and the MS/MS spectra generated by the exact masses and retention times was used to confirm the identified metabolites with significant changes (1.5-fold change, $p < 0.05$). The HMDB and KEGG databases were applied to find the altered metabolic pathway, which

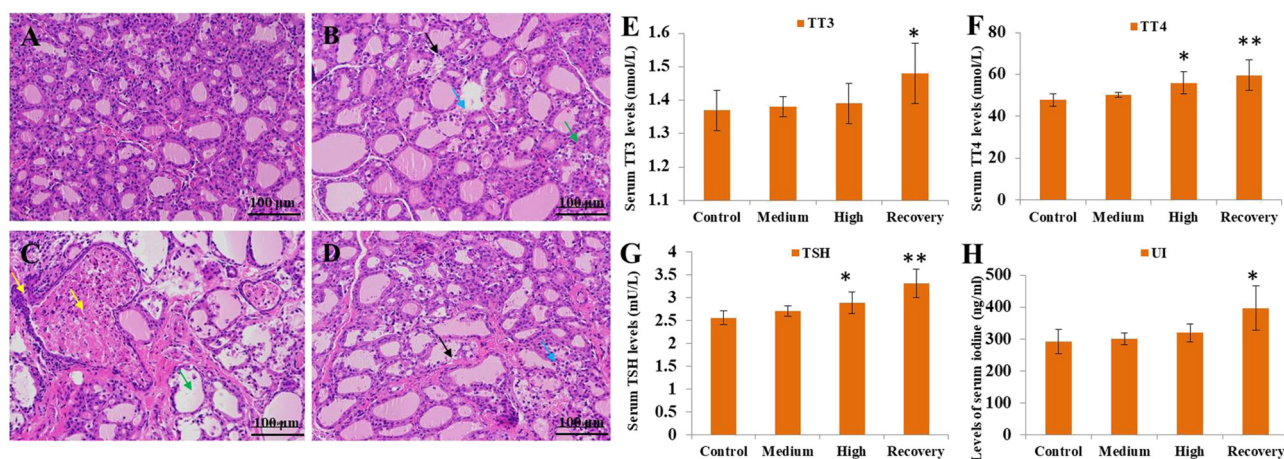


Fig. 1. Effect of PM_{2.5} exposure on thyroid histologic changes (A-D) and functional status (E-H). H&E staining of rat thyroid tissue. Infiltration of few macrophages into the lumen, and a few follicular epithelial cells were shed and disappeared in the M and H groups. The presence of diluted colloid staining and necrotic material filled the local follicles in the H group (200 \times , scale bars = 100 μ m) (A, Control; B, Medium; C, High; D, Recovery). Effects of various concentrations of PM_{2.5} on TT3, TT4, TSH, and UI levels in rat serum (TT3, E-Total triiodothyronine; TT4, F-Total thyroxine; TSH, G-thyroid-stimulating hormone; UI, H-urine iodine). The values are expressed as the mean \pm SEM. * $P < 0.05$ and ** $P < 0.01$ versus the control group.

was consistent with the identified microbial functional pathway. In addition, correlations between the changed gut microbes related to thyroid function indicators and shifted metabolites were conducted to establish the functional impacts of PM_{2.5} exposure on the thyroid.

2.9. Statistical analysis

All experiments data are expressed as mean ± standard deviation (SD). SPSS software (version 18.0, SPSS, Inc., Chicago, IL, USA) was used for statistical analysis. The homogeneity of variance was analyzed by Levene's test. The statistical differences between multiple groups were analyzed using one-way analysis of variance (ANOVA) followed by Tukey's test.

The statistical analysis of thyroid function was performed using GraphPad Prism version 5 (GraphPad Software, La Jolla, CA, USA). The correlation between gut microbiome and thyroid function or metabolome was analyzed using the Spearman correlation test. *P* < 0.05 was considered significant, and *P* < 0.01 was considered highly significant.

3. Results

3.1. Effect of PM_{2.5} exposure on male rats' thyroid histology

The histopathologic changes in thyroid tissue of male rats following PM_{2.5} exposure were evaluated using H&E staining. The C group displayed

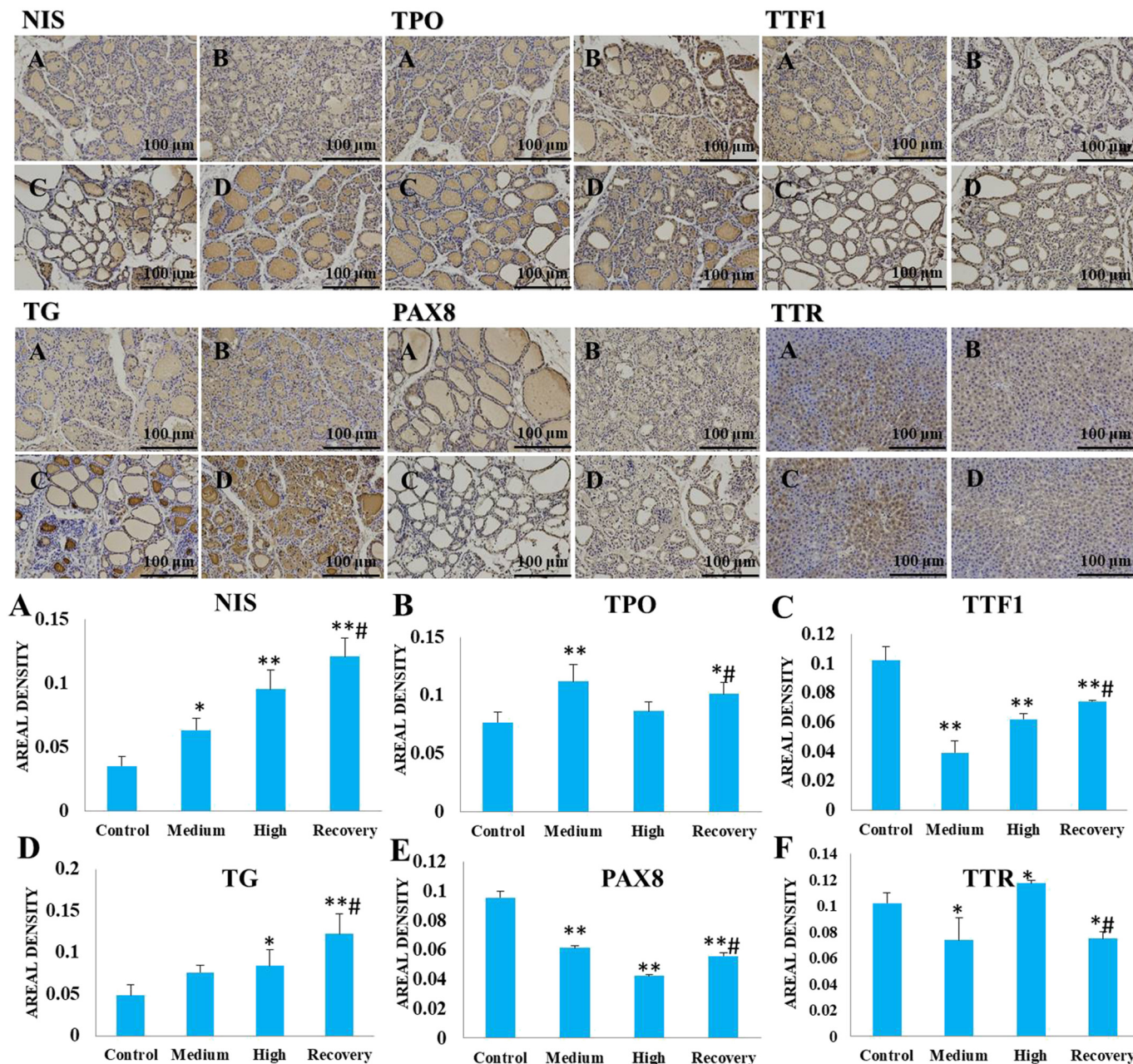


Fig. 2. Effect of PM_{2.5} exposure on the expression of thyroid hormone-related proteins. Protein expression levels of thyroid NIS, TPO, TTF1, TG, PAX8 and TTR were assessed by immunohistochemical analysis. Rats (*n* = 5/group) were treated with PM_{2.5} by passive pulmonary inhalation for 49 d. The development of brown and yellow color in the tissue sections indicated positive expression of the relevant target proteins. A: Control group, normal saline for 49 d; B: Medium-dose group, 15 mg/kg for 49 d; C: High-dose group, 30 mg/kg for 49 d. D: Recovery-dose group, 30 mg/kg for 35 d and no treatment for 14 d. NIS: Sodium iodide symporter; TPO: Thyroid peroxidase; TTF1: Thyroid transcription factor1; TG: Thyroglobulin; PAX8: paired box 8; TTR, Hepatic transthyretin. Magnification: 200 ×. The values are expressed as the mean ± SEM. **P* < 0.05 and ***P* < 0.01 versus the control group. #*P* < 0.05 versus the high-dose group.

normal cytoplasmic structure of follicular epithelial cells without any macrophage infiltration in the follicular lumen (Fig. 1A). In the M group, a few follicular epithelial cells were shed and disappeared and had vacuolated cytoplasm. In addition, a few macrophages might be infiltrated in the lumen (Fig. 1B). In the H group, a large number of thyroid follicular epithelial cells were exfoliated with more cells exhibited abnormal structures than those in the M group (Fig. 1C). Moreover, in the H group, colloid staining in a few follicles was diluted and even disappeared. The necrotic material filled the local follicles, and hyperplasia appeared in the surrounding epithelial cells. In recovery group, the follicle colloid staining was light, some immersed macrophages appeared, and some follicular epithelial cells were shed and lost (Fig. 1D). These results showed that PM_{2.5} dose-dependently induced infiltration of inflammatory cells.

3.2. Effect of PM_{2.5} exposure on levels of thyroid hormones in serum

The expression levels of thyroid hormones including TSH, total T3 (TT3), and total T4 (TT4), as well as urine iodine (UI) in serum were measured using ELISA to explore the influence of PM_{2.5} on thyroid function. Results showed that the serum TT4 and TSH levels in the H group were significantly higher than those in the C group, while no significant difference was observed between M and C groups (Fig. 1F and G). Moreover, upon exposure to PM_{2.5}, the serum TT3 and UI levels displayed an

increasing trend compared with the C group (Fig. 1E and H). However, both levels of thyroid hormones and UI in the recovery group were remarkably enhanced than the C group.

3.3. PM_{2.5} exposure affected expression of thyroid function-related proteins

The expression levels of thyroid-related proteins (PAX8, TG, TTF1, TPO, and NIS), pituitary TSHβ protein, and hypothalamus TRHR were examined to investigate the roles of the HPT axis in PM_{2.5}-induced thyroid dysfunction. The results indicated that compared to C group, PM_{2.5} significantly increased the NIS, TPO and TG levels in thyroid at d 49 ($P < 0.05$), and a significant decline in TTF1 and PAX8 was also observed. While the expression of these proteins was significantly increased in the recovery group at d 49 compared with the H group ($P < 0.05$) (Fig. 2). PM_{2.5} exposure led to a dramatic decrease in expression of hypothalamus TRHR in both M and H groups, as well as recovery group at 49 d. (Fig. S1). PM_{2.5} exposure induced a remarkable increase in pituitary TSHβ expression in both M and H groups at 49 d, while it went back to normal in the recovery group (Fig. S1). Moreover, both IHC and WB analyses revealed that compared with C group, the protein expression of liver TTR was dramatically decreased in PM_{2.5}-treated groups at d 49 ($P < 0.05$), while it presented a decreased trend in the recovery group compared to H group (Fig. S1).

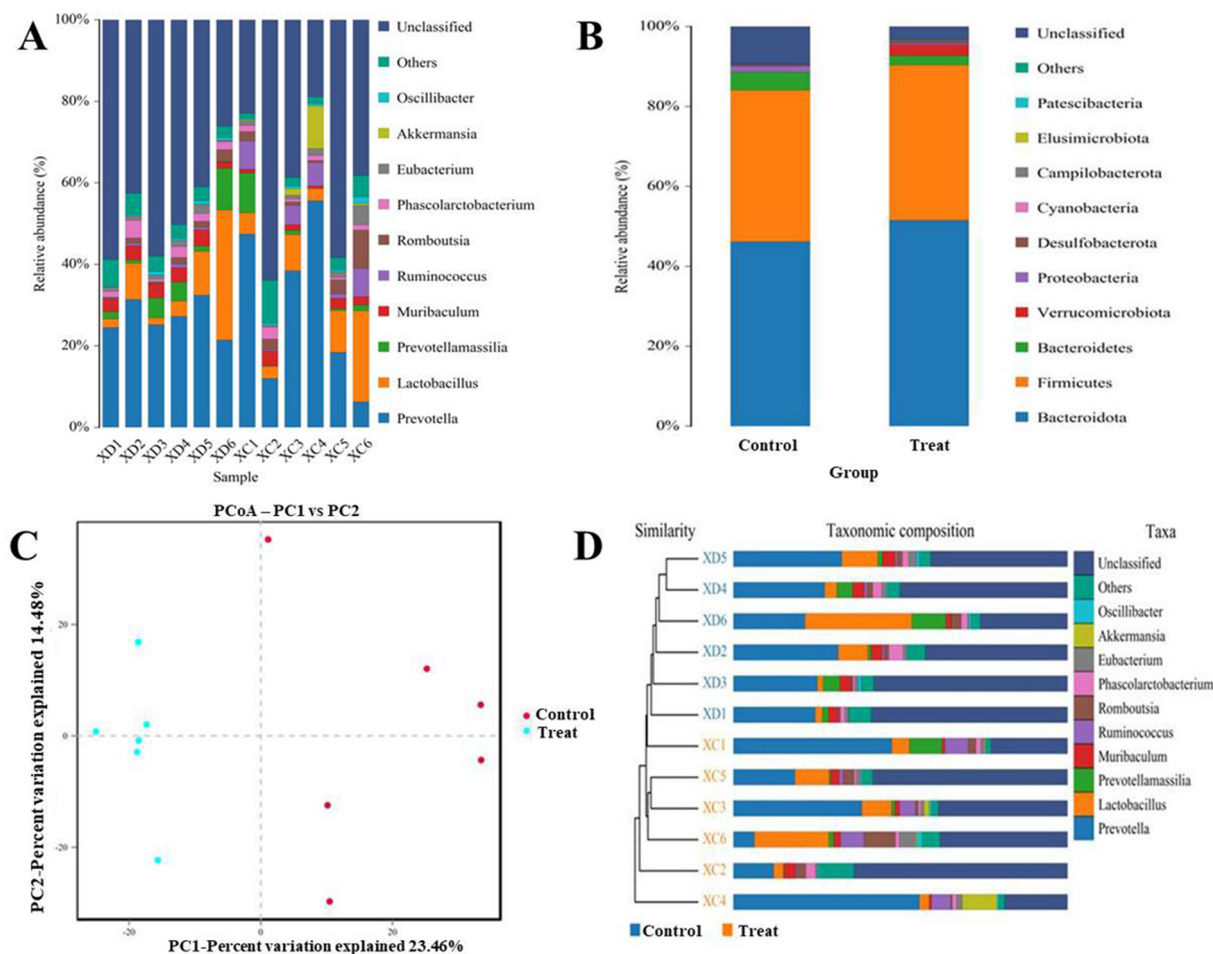


Fig. 3. PM_{2.5} exposure alters the composition of gut microbiome at the phylum level in rats revealed by 16S rRNA sequencing (each color represents one bacterial phylum). (A) Composition and relative abundance of bacterial phyla in all samples. (B) Composition and relative abundance of bacterial phyla in different groups. (C) The PCoA plot is generated of the R language tool based on the four distance matrices and explains the largest variance between all samples. (D) Community composition at the phylum level of each sample is shown with hierarchical clustering based on Weighted Unifrac Distance of OTU profiles. Note: Vertical seat represents Beta distance; the upper box diagram of “All Between” represents the Beta distance data of samples in all groups; the latter box diagram represents the Beta distance data of samples in different groups. Horizontal clustering is sample information, while vertical clustering is species information. The left cluster tree is the phylum cluster tree. In the middle is the heat map. The product level clustering tree: the closer the samples are, the shorter the branch length is, suggesting that the species composition of the two samples is more similar.

3.4. Effect of PM_{2.5} exposure on community diversity and gut microbiome richness

The influence of PM_{2.5} exposure on gut microbiome was evaluated using 16S rRNA gene sequencing (Table S2). The alpha diversity index was applied to analyze the community diversity and richness (Fig. S2A and B). Results showed that compared with C group, PM_{2.5} exposure induced increased shannon index and decreased simpson index, indicative of an increased gut microbiome diversity caused by PM_{2.5}. Meanwhile, compared with C group, the richness estimator chao1 and ACE were significantly promoted in the PM_{2.5}-treated group (Fig. S2C and D).

3.5. Effect of PM_{2.5} exposure on composition of gut microbiome

Totally 1286 OTUs were identified in the publicly available sequences from the SILVA 132 repository. The proportions of annotated OTUs at kingdom, phylum, class, order, family, genus, and species levels were 98.22%, 73.34%, 72.12%, 68.72%, 61.99%, 35.49%, and 12.40%, respectively. At the phylum level, *Bacteroidota* was the predominant phylum in the gut microbiome of rats, with a total abundance of nearly 90%, followed by the *Verrucomicrobiota*, *Proteobacteria*, *Elusimicrobiota*, *Cyanobacteria*, *Patescibacteria*, *Desulfobacterota*, *Firmicutes* and *Bacteroidetes*. These microbes exhibited differences upon PM_{2.5} exposure. Among them, *Cyanobacteria*, *Bacteroidetes*, and *Proteobacteria* had a quite low relative abundance in the PM_{2.5}-treated group, which decreased with increasing PM_{2.5} concentration. In contrast, the relative abundance of *Verrucomicrobiota*, *Elusimicrobiota*, *Patescibacteria*, *Desulfobacterota*, *Firmicutes* and *Bacteroidota* in the PM_{2.5}-treated group was significantly higher than that in the C group (Fig. 3A and B).

The PCoA plot displayed a distinct structure of gut microbiome induced by PM_{2.5} exposure compared with C group (Fig. 3C). The PM_{2.5}-treated group was well separated, with principle components PC1 and PC2 contributing to 23.46% and 14.48% variation, respectively. Moreover, the hierarchical clustering analysis using the unweighted pair group method with arithmetic mean (UPGMA) showed that most of the PM_{2.5} treated and control samples clustered in their own groups (Fig. 3D).

3.6. Correlations between gut microbial species and clinical indices and functional protein in PM_{2.5}-induced thyrotoxicity rats

To clarify the pathological significance of the altered intestinal bacteria in PM_{2.5}-induced thyrotoxicity rats, the relationships between the relative abundances of the intestinal bacteria and clinical features (serum levels of TT3, TT4 and TSH) and functional protein (thyroid tissue levels of NIS, TPO, TTF1, TG, PAX8 and TTR) of PM_{2.5}-induced thyrotoxicity rats were analyzed using the Spearman's rank correlation coefficient method. Results indicated that *Firmicutes*, *Bacteroidota*, and *Bacteroidetes* were negatively correlated with the serum level of TSH. In addition, *Bacteroidota* were negatively correlated with those of TT3 and TT4. Moreover, *Cyanobacteria* was negatively correlated with those of TT4 at the phylum level (Fig. 4A). At the phylum level, *Bacteroidetes*, *Proteobacteria* and *Bacteroidota* were positively correlated with thyroid tissue levels of NIS and TG, and *Bacteroidetes* was negatively correlated with those of TTF1 and PAX8. *Proteobacteria* and *Bacteroidota* were negatively correlated with those of TTF1 (Fig. 4C). At the genus level, *Allobaculum* was negatively correlated with the serum level of UI, *Eubacterium* was negatively correlated with the serum level of TSH, *Lactobacillus* and *Muribaculum* were negatively correlated with the serum level of TT3, and *Candidatus-Obcuribacter* and *Lactobacillus* were negatively correlated with the serum level of TT4 (Fig. 4B). At the genus level, *Lactobacillus*, *Prevotella*, *Muribaculum*, *Ileibacterium*, *Escherichia* were positively correlated with thyroid tissue levels of NIS and TG. *Parasutterella* and *Lactobacillus* were positively correlated with those of NIS and TTF1, respectively. In addition, *Prevotella* and *Muribaculum* were negatively correlated with those of TTF1 and PAX8. *Parasutterella* and *Escherichia* were negatively correlated with those of TTF1 (Fig. 4D).

3.7. Imputed microbiome function and phenotype prediction induced by PM_{2.5} exposure

Given the structural differences in intestinal bacteria displayed by PERMANOVA/Anosim analysis (Fig. 5A), we next explore whether PM_{2.5}-induced thyrotoxicity leads to functional changes in the microbiome. As shown by Fig. 5B, the biomarkers with statistically significant differences

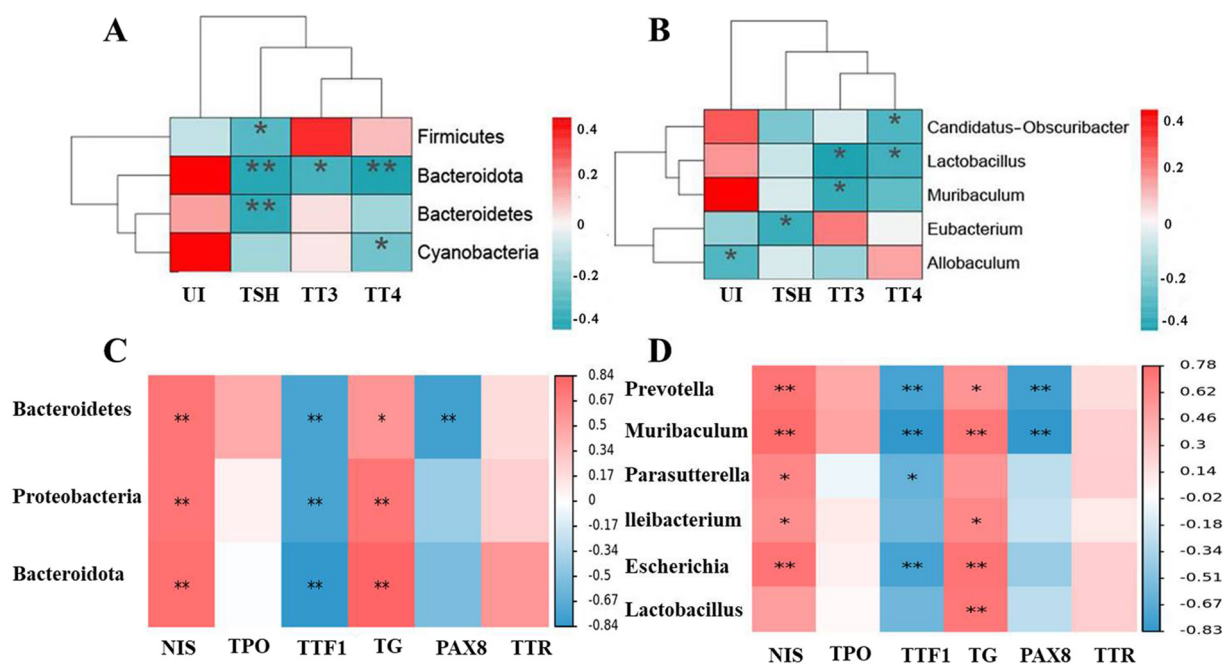


Fig. 4. Correlations between intestinal bacteria and clinical indicators or functional proteins of PM_{2.5}-induced thyrotoxicity in rats. Heatmap of correlations between clinical indicators or functional proteins of PM_{2.5}-induced thyrotoxicity in rats and the abundances of the intestinal bacterial phyla (A, C) and genera (B, D). The color bars with numbers indicate the correlation coefficients. The false discovery rate (FDR)-adjusted P-values by t-test are shown by asterisks (*: corrected P < 0.05; **: corrected P < 0.01).

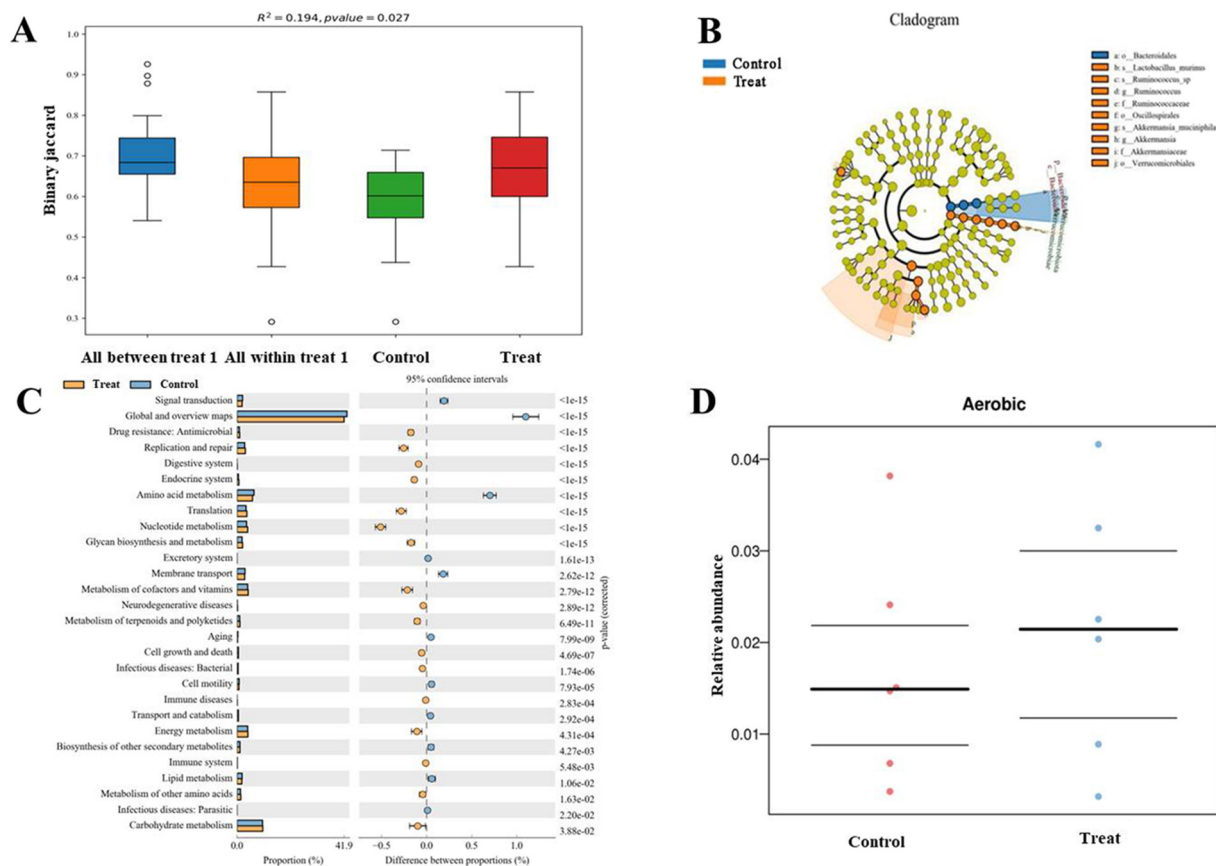


Fig. 5. Imputed metagenomic differences between the PM_{2.5}-treated and control groups. (A) Beta diversity difference between the treated and control groups. (B) Taxonomic cladogram obtained using linear discriminant analysis (LDA) effect size (LEfSe) analysis of the 16S sequences. (C) The significant differences in metagenomic functions of PM_{2.5}-induced thyrotoxicity in rats compared with control individuals (corrected $P < 0.05$ and confidence intervals = 95%). (D) BugBase phenotype prediction diagram. The important metagenomic functions are marked with rectangles (corrected $P < 0.05$ and confidence intervals = 95%). This analysis was performed by software PICRUSt. Note: The figure shows the species whose LDA Score is greater than the set value (default setting is 4.0). The length of the bar chart represents the impact size of different species (i.e., LDA Score), and different colors represent the species in different groups.

were screened by Line Discriminant Analysis (LDA) Effect Size as described previously. The Bray-Curtis distance-based community analysis revealed an evident separation between PM_{2.5}-treated and control groups, indicating these two groups exhibited significant difference in metabolic function composition. The KEGG pathways with the largest difference included metabolism of terpenoids and polyketides, amino acid metabolism, carbohydrate metabolism, lipid metabolism, nucleotide metabolism, endocrine system, energy metabolism, and nervous system, exhibiting lower relative abundance in PM_{2.5}-treated group than C group (Fig. 5C). Moreover, the aerobic level was markedly enhanced in PM_{2.5}-induced thyrotoxicity rats presented in BugBase phenotype prediction diagram (Fig. 5D).

3.8. Effect of PM_{2.5} exposure on the urine metabolic profile, biomarker identification and metabolic pathway screening

The metabolite profiles of the urine samples were explored using LC-MS. The 3D PCA Plot showed that the metabolites of both PM_{2.5}-treated and control groups were well separated, with 50.36%, 7.59% and 6.16% variation attributed to the principle components PC1, PC2 and PC3, respectively (Fig. 6A). The compounds responsible for the differences between different groups were identified using an OPLS-DA model, with OPLS-DA scores indicating that the control and PM_{2.5}-treated groups were dispersed in two different regions. Goodness of fit values and predictive ability values (treated vs control group: $R^2X = 0.836$, $R^2Y = 0.873$, $Q^2Y = 0.462$, and $P \leq 0.05$) showed that the OPLS-DA model had a good fit with excellent predictive power (Fig. 6B). The R^2 and Q^2 values of the model after Y substitution were less than those in the

original model, suggesting that the model was appropriate for screening of metabolites according to Variable Importance in the Projection (VIP) (Fig. 6C).

Totally 1798 differential metabolites were identified in the control versus treated groups. Among them, 8 metabolites decreased while 1790 metabolites increased in the PM_{2.5}-treated group compared with control group (Fig. 6D and F). The metabolites exhibiting different levels were further screened using VIP (Susanne et al., 2007). Metabolites with fold change ≥ 1.5 or ≤ 0.5 , $VIP \geq 1.0$, and $P \leq 0.05$ were considered as differential metabolites, including 37 biomarkers in positive mode (Table S3), and 23 biomarkers in negative mode (Table S4). The identified main differential metabolites were further quantitatively and qualitatively analyzed, and the top 20 differential metabolites between control and treated groups were screened by Linear discriminate analysis (LDA) effect size analysis (Fig. 6E).

The Kyoto Encyclopedia of Genes and Genomes (KEGG) database was used to further analyze the metabolic pathways affected by PM_{2.5} exposure. The results indicated that these metabolites included carboxylic acids and derivatives, 5'-deoxyribonucleosides, fatty acyls, steroids and steroid derivatives, nucleoside and nucleotide analogues, among others (Fig. 7A), which represent key metabolic pathways including thyroid hormone synthesis, arginine and proline metabolism, tryptophan metabolism, primary bile acid biosynthesis, cysteine and methionine metabolism, histidine metabolism, nicotinate and nicotinamide metabolism, bile secretion, D-glutamine and D-glutamate metabolism, beta-alanine metabolism, glutathione metabolism, glyoxylate and dicarboxylate metabolism, ascorbate and aldarate metabolism, as well as ABC transporters (Fig. 7B).

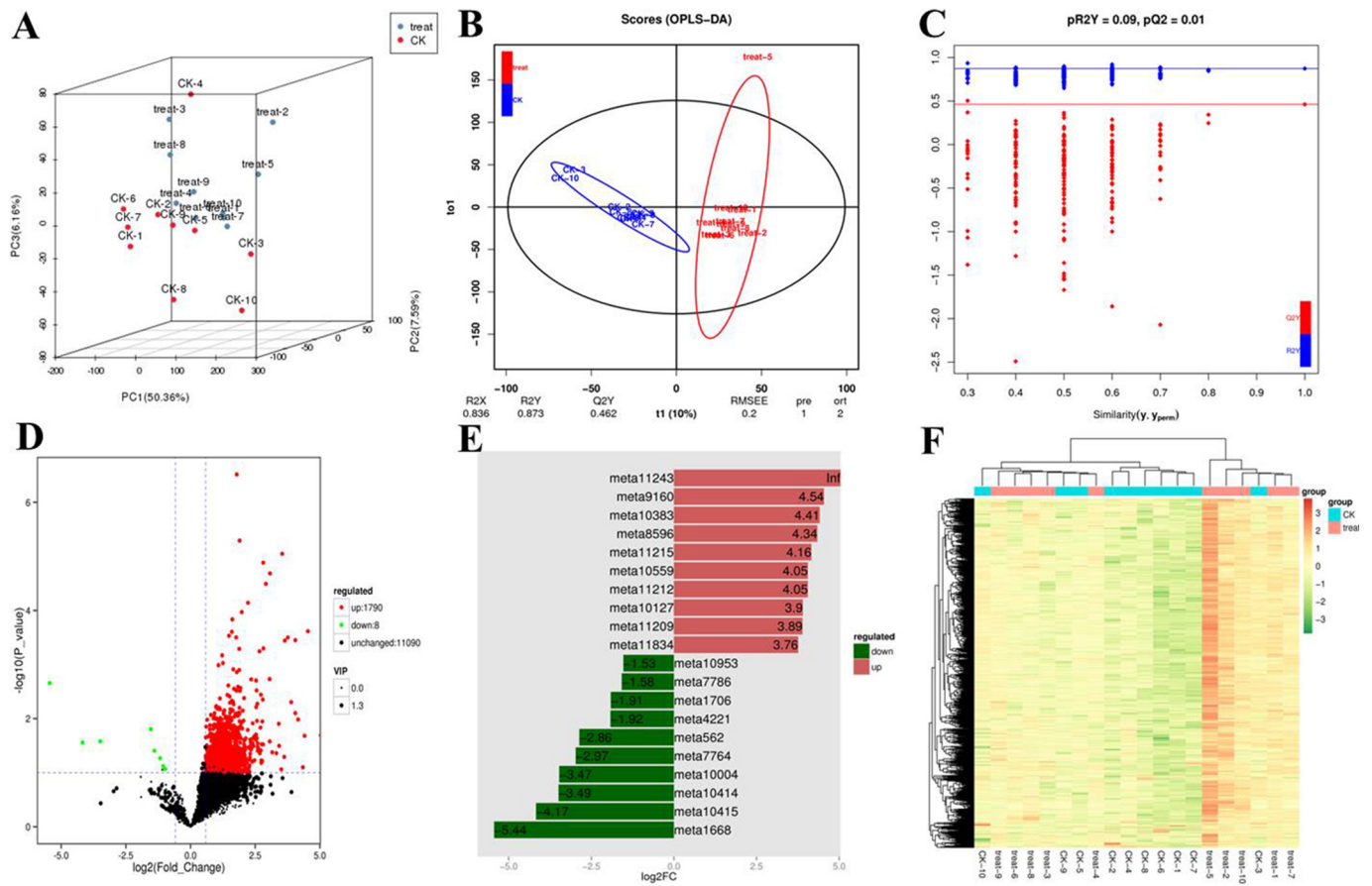


Fig. 6. PCA scatter plot of the metabolite profile and variation characteristics of various metabolites in the urine treated by PM_{2.5}. The control group was separated from PM_{2.5} treated group (A). OPLS-DA analysis of the metabolite profile. OPLS-DA score plot (B) and OPLS-model test chart (C) show good discrimination between the treated and control groups, R²X = 0.836, R²Y = 0.873, Q² = 0.462, and P < 0.05. Volcano Plot showing differential metabolites between the control and treated groups (D). Linear discriminant analysis (LDA) effect size analysis of top 20 differential metabolites between the treated and control groups (E). Hierarchical clustering heat map analysis of differential metabolites between the treated and control groups (F). Each column represents a sample and each row depicts a metabolite. The color of each section corresponds to a concentration value of each metabolite calculated by peak area normalization method (red, upregulated; green, downregulated). The data set was screened using variable importance for projection (VIP) values >1, values of fold change ≥ 2 or ≤ 0.5, p-value <0.05, in the urine metabolites.

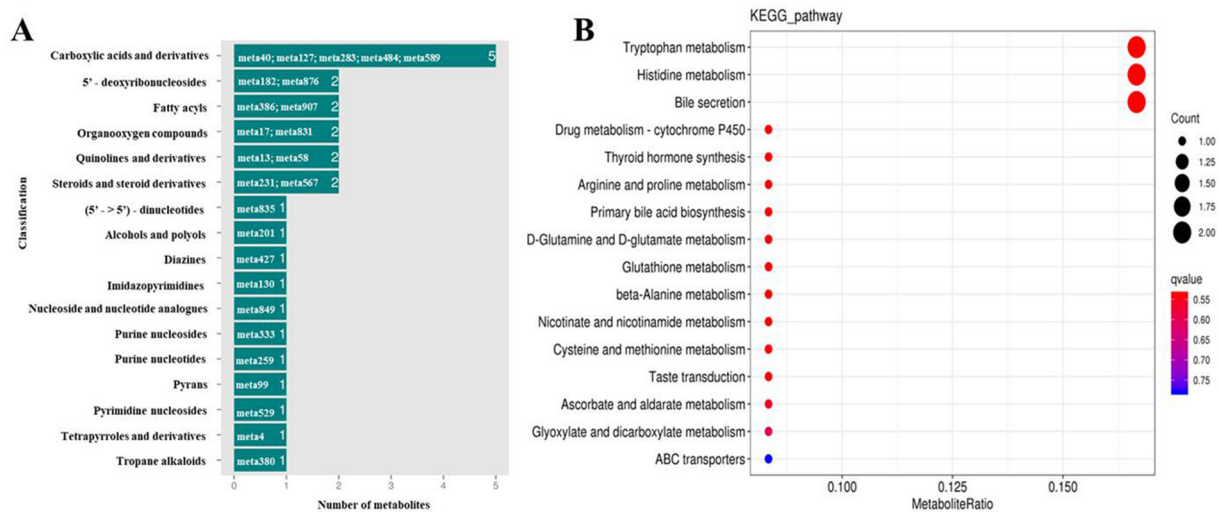


Fig. 7. HMDB classification of different metabolites in each group (A) and pathway analysis of differential metabolites between the PM_{2.5}-treated and control groups (B). Urine metabolic alterations of the most relevant pathways induced by PM_{2.5} were analyzed using the MetaboAnalyst 3.0., and the significantly enriched pathways are displayed by a bubble plot (p < 0.05, Fisher's exact test).

3.9. Correlations between urine metabolites and clinical indices and functional protein in PM_{2.5}-induced thyrotoxicity rats

To further clarify the biological significances of the altered urine metabolites in PM_{2.5}-induced thyrotoxicity rats, the relationships between the relative abundances of the urine metabolites and clinical features (serum levels of TT3, TT4 and TSH) and functional protein (thyroid tissue levels of NIS, TPO, TTF1, TG, PAX8 and TTR) of PM_{2.5}-induced thyrotoxicity rats were analyzed using the Spearman's rank correlation coefficient method. Results indicated that 5-Aminopentanoic acid, 2-Pyrrolidinone, PI-18-0-16-0, glycylylprolylhydroxyproline, and chlorogenic acid, etc. were positively correlated with thyroid tissue levels of TTF1 and PAX8. Serylaspatic acid, 5-Pminopentanoic acid, 2-pyrrolidinone, PI-18-0-16-0, chlorogenic acid, and kynurenic acid, etc. were negatively correlated with those of NIS and TSH. Citric acid, 2-Pyrrolidinone, kynurenic acid, PI-18-0-16-0, and l-Proline, etc. were negatively correlated with those of TT4. Gamma-Glutamylleucine, glycylylprolylhydroxyproline, chlorogenic acid, and glucosylgalactosyl hydroxyllysine, etc. were negatively correlated with those of TG in positive ion mode (Fig. 8A). In negative ion mode, creatinine was negatively correlated with those of TT3 and TT4. Kynurenic acid was negatively correlated with the levels of TT3, UI and NIS. N-Acetyl-L-arginine was negatively correlated with the levels of TSH and NIS. Glutathione and L-Gulonolactone were negatively correlated with the level of NIS and TTR, respectively. Naringenin-4-O-glucuronide and glutathione were positively correlated with thyroid tissue levels of PAX8. 2-Hydroxy-3-methylbutyric-acid, N-Acetyl-L-arginine and glutathione were positively correlated with those of TTF1 (Fig. 8B).

3.10. Potential correlations between gut microbiome and urine metabolites

Based on the differences in metabolites and gut microbiome between the control and PM_{2.5}-treated groups, the functional correlations between

the alterations in metabolite profiles and gut microbiome were explored by calculation of the Spearman's correlation coefficient. A significant correlation ($r = 0.8$; $P < 0.05$) was observed between the alterations in metabolite profiles and the perturbed gut microbiome at the genus (Fig. 8C and D) and phylum levels (Fig. 8E and F). Fig. 8 lists several typical gut microflora-related metabolites that are highly correlated with specific gut bacteria to demonstrate the functional correlation between the gut microbiome and metabolites. The results showed that the abundances of some bacterial families, including *Lactobacillaceae*, *Erysipelotrichaceae*, *Prevotellaceae* and *Muribaculaceae* highly correlated with a few metabolites (Fig. 8), vice versa. For example, the D-Glutamic acid level positively correlated with the abundance of *Enterobacteriaceae* ($r = 0.8377$, $p = 0.000670$), *Prevotellaceae* ($r = 0.8707$, $p = 0.000228$), and *Muribaculaceae* ($r = 0.9072$, $p = 0.000046$); the urocanic acid level positively correlated with the abundance of *Erysipelotrichaceae* ($r = 0.8298$, $p = 0.000838$) and *Lactobacillaceae* ($r = 0.8469$, $p = 0.000508$); the Glutathione level positively correlated with the abundance of phylum including *Bacteroidota* ($r = 0.8071$, $p = 0.001504$); the Kynurenic acid level positively correlated with the abundance of several phyla including *Firmicutes* ($r = 0.8505$, $p = 0.000456$), *Bacteroidota* ($r = 0.9380$, $p = 0.000007$), *Elusimicrobiota* ($r = 0.8775$, $p = 0.000176$), and *Campilobacterota* ($r = 0.8716$, $p = 0.000221$); the D-Glutamic acid level positively correlated with the abundance of several phyla including *Firmicutes* ($r = 0.8268$, $p = 0.000910$), *Bacteroidota* ($r = 0.9072$, $p = 0.000046$), and *Proteobacteria* ($r = 0.8377$, $p = 0.000670$); the Citric acid level positively correlated with the abundance of several phyla including *Firmicutes* ($r = 0.8356$, $p = 0.000710$), *Elusimicrobiota* ($r = 0.8555$, $p = 0.000386$), *Bacteroidota* ($r = 0.9059$, $p = 0.000049$), *Campilobacterota* ($r = 0.8511$, $p = 0.000445$) and *Cyanobacteria* ($r = 0.8175$, $p = 0.001161$); the Taurocholic acid level positively correlated with the abundance of *Elusimicrobium* ($r = 0.9741$, $p = 0.000000$), *Muribaculum* ($r = 0.9886$, $p = 0.000000$), *Candidatus_Obscuribacter* ($r = 0.8423$, $p = 0.000585$), *Eubacterium* ($r =$

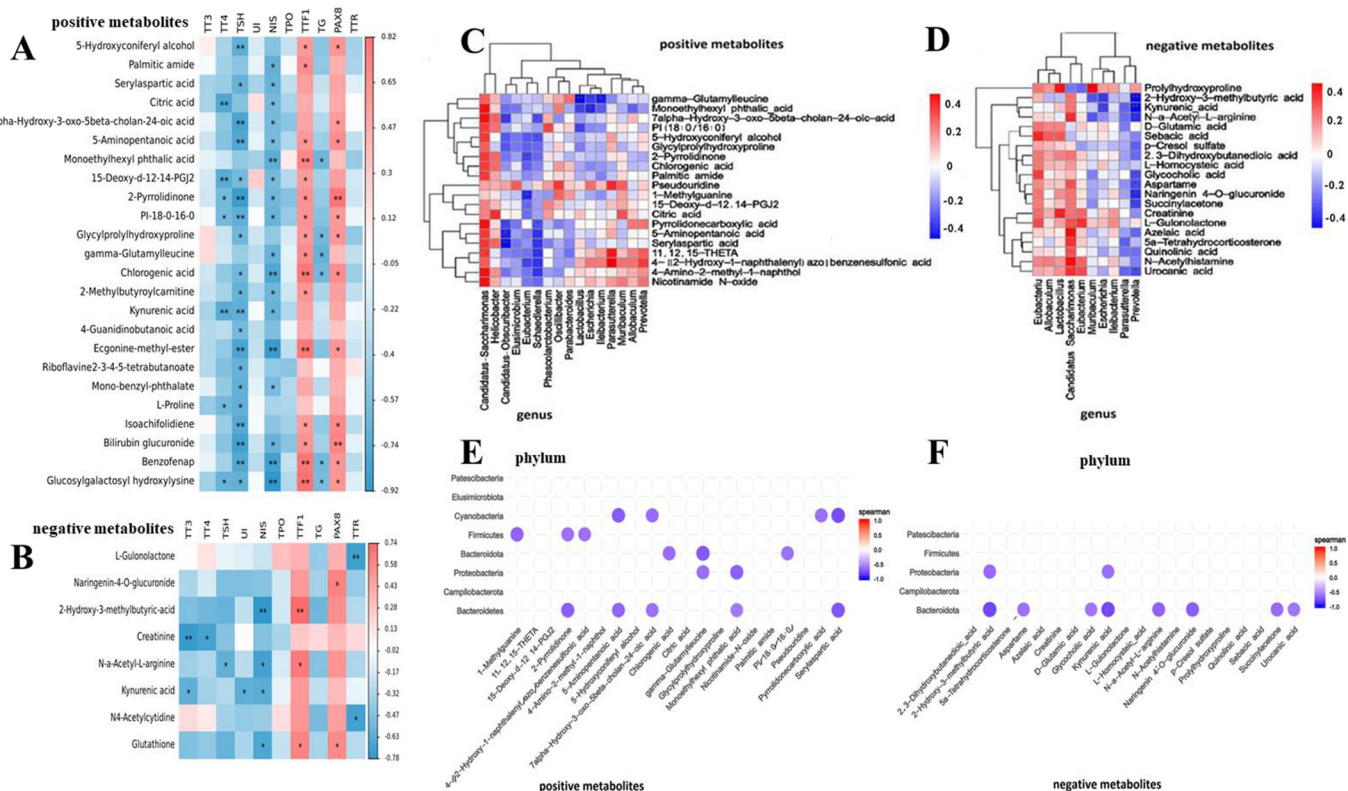


Fig. 8. Correlations analysis between clinical indicators or functional proteins and metabolites (A, B) and conjoint analysis of microbiota and metabolites (C-E). Correlation map (A, B) showing the functional correlation between clinical indicators or functional proteins and altered urine metabolites in positive and negative ion mode. Correlation map (C, D) and plot (E, F) showing the functional correlation between perturbed gut bacteria genera or phyla and altered urine metabolites in positive and negative ion mode. Red represents the positive correlation, and blue or light blue represents the negative correlation.

0.9237, $p = 0.000017$), and *Parabacteroides* ($r = 0.8813$, $p = 0.000150$), whereas it negatively correlated with the abundance of *Prevotella* ($r = -0.8070$, $p = 0.001509$); the 2-Pyrrolidinone level positively correlated with the abundance of *Elusimicrobium* ($r = 0.8811$, $p = 0.000153$), *Muribaculum* ($r = 0.9016$, $p = 0.000062$), *Candidatus_Obscuribacter* ($r = 0.8295$, $p = 0.000846$), *Eubacterium* ($r = 0.9133$, $p = 0.000033$), *Parabacteroides* ($r = 0.8110$, $p = 0.001371$), *Helicobacter* ($r = 0.8694$, $p = 0.000239$) and *Prevotella* ($r = 0.8175$, $p = 0.001165$); the gamma-Glutamylleucine level positively correlated with the abundance of *Elusimicrobium* ($r = 0.9310$, $p = 0.000011$), *Muribaculum* ($r = 0.9224$, $p = 0.000019$), *Candidatus_Obscuribacter* ($r = 0.8046$, $p = 0.001598$), *Eubacterium* ($r = 0.8854$, $p = 0.000128$), *Parabacteroides* ($r = 0.9515$, $p = 0.000002$), and *Helicobacter* ($r = 0.9222$, $p = 0.000020$), whereas it negatively correlated with *Lactobacillus*, *Escherichia*, and *Ileibacterium*. Taken together, these results suggest that PM_{2.5} exposure induces a significant taxonomic perturbation in the gut microbiome, which in turn substantially alters the metabolomic profile of the gut microbiome, as evidenced by changes of diverse gut microflora-related metabolites. In addition, the alterations in the aforementioned gut microbiome and gut microflora-related metabolites were significantly correlated with changes in thyroid function indexes.

4. Discussion

Thyroid cancer is the leading endocrine cancer (Bray et al., 2018), with increasing incidence in the past decades (Cai and Liu, 2021) in the USA (Kitahara and Sosa, 2016) and Asia (Ahn et al., 2016). Thyroid disease can affect all stages of life (Wang et al., 2020). The atmosphere level of PM_{2.5} gradually increases with increasing urbanization and industrialization, which enhances the risk of diseases including endocrine system diseases (Darbre, 2018). The toxic effects of PM_{2.5} and related mechanisms have been investigated (Dong et al., 2021a; Riggs et al., 2020). However, the mechanism underlying PM_{2.5}-induced thyroid injury remains unclear.

Combination of metabolomics, microbiome and the related metabolites can be used to understand the disease development mechanisms (Li et al., 2020; Lin et al., 2021). Recent studies reported the impact of PM_{2.5} exposure on gut microbiome (Zhao et al., 2021) and the potential relationship between gut microbiome and thyroid disease (Virili et al., 2021). However, no study combines metabolic profile and microbiome analyses to investigate PM_{2.5} exposure-induced thyrotoxicity. Herein, we constructed a rat thyroid injury model via intratracheal instillation of PM_{2.5}. H&E staining showed infiltration of few macrophages into the lumen, disappeared follicular epithelial cells, diluted colloid staining and the necrotic material in the local follicles in the M and H groups, indicating the presence of inflammatory thyroid injury (Wang et al., 2017), consistent with previous study showing that PM_{2.5} exposure significantly resulted in light color colloid dyeing, inducing exfoliated follicular epithelial cells, macrophages and inflammatory cells (Kroemer et al., 2009). ELISA analysis indicated that the serum TT4 and TSH levels were remarkably enhanced following PM_{2.5} exposure. Considering that iodine is an important ingredient in the synthesis of thyroid hormones (Ren et al., 2021), we concluded that PM_{2.5} induced thyroid injury by affecting thyroid hormone levels via impacting the expression of thyroid functional proteins. Therefore, we further analyzed thyroid functional proteins in male rats and observed increased levels of NIS, TPO, TG and TTR, but decreased levels of TTF-1 and PAX-8 after PM_{2.5} exposure. These results suggest that PM_{2.5} exposure may affect the secretion, biosynthesis and biotransport of thyroid hormones by interfering with the expression of the above functional proteins via the HPT axis, thus leading to thyroid dysfunction. This is consistent with our previous conclusions on the mechanism of thyroid injury in female rats (Dong et al., 2021a). But the specific regulatory mechanism and cause for the abovementioned changes are still unclear. Studies showed that air pollutants may influence the relative abundance of gut bacteria (Zhao et al., 2021). However, whether air pollutants-induced potential composition and functional alterations in gut microbiome are associated with thyroid function remains unclear. The gut microbiome has been demonstrated to even impact the whole

body health by gut-thyroid axis (Lerner et al., 2017). Therefore, this study aimed to explore whether residential based estimate of PM_{2.5} exposure was associated with the gut microbiome in rats and its relationship with thyrotoxicity.

This study, for the first time, utilized LC-MS-based metabolomics profiling analysis and high-throughput 16S rRNA gene sequencing to explore the influence of PM_{2.5} exposure on gut microbiome and metabolic profile related to thyroid function alterations. The results revealed that PM_{2.5} exposure caused a marked change in rat gut microbiome composition, and the gut microbiome in PM_{2.5}-treated group exhibited a higher community diversity and richness (α -diversity) than the control group, consistent with previous report by Zhao et al. (Zhao et al., 2021). First, Shannon, Chao1 and Ace were higher, but Simpson was lower in PM_{2.5}-induced thyrotoxicity, suggesting the bacterial diversity and richness in guts of PM_{2.5}-induced thyrotoxicity rats were increased, consistent with previous report on gut microbiota in hypothyroidism and hyperthyroidism patients (Su et al., 2020). In addition, we observed that the major differential intestinal bacteria (*Firmicutes*, *Bacteroidota*, *Bacteroidetes*, and *Cyanobacteria*) could represent biomarkers for clarifying PM_{2.5}-induced thyrotoxicity mechanism. They were negatively correlated with thyroid function indicators (TT3, TT4, and TSH) and positively correlated with the serum UI level at the phyla level. Additionally, the altered bacteria of PM_{2.5}-induced thyrotoxicity rats including *Candidatus-Obscuribacter*, *Lactobacillus*, *Muribaculum*, *Eubacterium*, and *Allobaculum*, which were negatively correlated with serum TT4, TT3, TSH, and UI levels at the genera level. Previous studies showed that dysbacteriosis could influence thyroid hormone synthesis and metabolism (DiStefano et al., 1993), and deiodinate thyroid hormones, thereby impacting the levels of these hormones in serum (Fekete et al., 2004). Moreover, the relationships analysis results about the altered intestinal bacteria and functional protein (thyroid tissue levels of NIS, TPO, TTF1, TG, PAX8 and TTR) further supported evidence that the above-mentioned intestinal bacteria could affect the thyroid function and the HPT axis of PM_{2.5}-induced thyrotoxicity rats. These results suggest that PM_{2.5} exposure alters the structure of gut microbiome and leads to thyroid injury.

In fact, the correlation between PM_{2.5} exposure and thyroid injury was reported previously (Irizar et al., 2021); the gut-thyroid link and gut microbiomes might function as intermediaries to promote individual susceptibility to inhaled PM_{2.5}. The gut microbiome has been demonstrated to interact with the gut-thyroid link (Li et al., 2021a), suggesting that PM_{2.5} exposure-induced gut microbiome perturbations could be an etiological pathway leading to thyroid injury. Moreover, PM_{2.5} and its main constituents- black carbon (BC), organic matter (OM), nitrate (NO₃(-)), ammonium (NH₄(+)) and sulfate (SO₄(2-)) influence the maternal and neonatal thyroid function and in turn induce changes in the distribution and structure of gut microbiota, a possible mechanism by which PM_{2.5} exposure alters gut microbiome (Wang et al., 2019). Moreover, these perturbed gut bacteria found in this study were closely related to alterations of substantial gut microflora-associated metabolites, suggesting that PM_{2.5} exposure both disturbs gut bacteria at abundance level and alters the metabolomic profile of the gut microbiome, thereby disturbing host metabolite homeostasis. The imputed metagenomic differences between control and PM_{2.5}-treated groups were involved in endocrine system, amino acid metabolism, nervous system, nucleotide metabolism, lipid metabolism, energy metabolism and glycan biosynthesis metabolism. These results might shed new light on PM_{2.5} exposure-induced perturbations of the gut microbiome, a possible novel mechanism for environmental chemical-induced thyroid disease. However, the deep reasons between the PM_{2.5}-induced gut microbiota changes and thyroid dysfunction requires further study.

To further investigate the causes of changes in the biological pathways of bacteria, liquid chromatography-coupled metabolomics techniques were applied to explore the key regulatory mechanisms for the aforementioned altered pathways. In this study, PCA, OPLS-DA and hierarchical clustering heat map showed that PM_{2.5} exposure caused significant changes in urine metabolic profile and some potential biomarkers were identified in

negative and positive ion mode. The levels of metabolites including urocanic acid, D-Glutamic acid, taurocholic acid, glutathione, kynurenic acid, N-Acetylhistamine, creatinine, 2,3-Dihydroxybutanedioic acid, aspartame, 5-Aminopentanoic acid, citric acid, o-propanoyl-carnitine, PI(18:0/16:0), 11,12,15-THETA, Nicotinamide N-oxide, 2(N)-Methyl-norsalsolinol, calcitriol, S-Adenosylmethionine, and 4-Guanidinobutanoic acid in the PM_{2.5}-treated groups increased significantly compared with those in the control group, whereas the prolylhydroxyproline level exhibited a decreasing trend. Glutathione is an intermediate for thyroid hormone synthesis. Arginine and proline metabolism, glutathione metabolism, lysine degradation, and glyoxylate and dicarboxylate metabolism are involved in energy metabolism. The decrease in levels of glutathione, citric acid, and 5-Aminopentanoic acid in the PM_{2.5}-treated groups revealed that PM_{2.5} exposure impacted the energy consumption and TCA cycle, indicative of PM_{2.5} exposure-induced disturbance of thyroid function, similar with previous report (Xu et al., 2019). Further analysis with KEGG database showed that differential metabolites were involved in thyroid hormone synthesis, primary bile acid biosynthesis, arginine and proline metabolism, tryptophan metabolism, histidine metabolism, bile secretion, cysteine and methionine metabolism, nicotinate and nicotinamide metabolism, beta-Alanine metabolism, glutathione metabolism, D-Glutamine and D-glutamate metabolism, ascorbate and aldarate metabolism, glyoxylate and dicarboxylate metabolism, as well as ABC transporters. The screened differential metabolites in dicarboxylate and glyoxylate metabolism demonstrated that PM_{2.5} exposure disturbed energy metabolism. Tryptophan metabolism, nicotinate and nicotinamide metabolism, primary bile acid biosynthesis, thyroid hormone synthesis and histidine metabolism exert modulating function in neuroendocrine system disorder (Robitaille, 1995). Moreover, D-Glutamine and D-glutamate metabolism generates oxygen free radicals, which play a key role in PM_{2.5}-induced oxidative stress. Fernandez-Pastor et al. showed that D-Glutamine and D-glutamate metabolism disorder is correlated with altered thyroid function (Fernandez-Pastor et al., 1983). PM_{2.5} exposure-induced perturbed arginine and proline metabolism in thyroid injury was first reported in this study. Amino acids are closely associated with gut-thyroid axis activation and inflammation (van der Boom et al., 2020), so amino acid metabolic disorder might induce thyroid immune disorders and enhance inflammation. Furthermore, the correlation analysis results about the urine metabolites and clinical features (serum levels of TT3, TT4 and TSH) and functional protein (thyroid tissue levels of NIS, TPO, TTF1, TG, PAX8 and TTR) further testified that the above-mentioned metabolites and their pathways could regulate the thyroid function and the HPT axis of PM_{2.5}-induced thyrotoxicity rats. In summary, the metabolomics results may help to clarify the thyrotoxicity mechanism caused by PM_{2.5} treatment in rats.

To further prove that PM_{2.5} affects the flora and thus changes thyroid homeostasis through the above-mentioned altered biomarkers, the functional conjoint analyses between perturbed gut bacteria at genera or phyla level and altered urine metabolites in positive and negative ion mode were conducted in this study. We found that the altered urine metabolites exhibited significant correlations with gut microbiota. *Lactobacillaceae*, *Erysipelotrichaceae*, *Prevotellaceae* and *Muribaculaceae* were closely associated with the levels of multiple metabolites in the host. For instance, the urocanic acid level positively correlated with the abundance of *Erysipelotrichaceae* and *Lactobacillaceae*. The D-Glutamic acid level positively correlated with the abundance of *Enterobacteriaceae*, *Prevotellaceae*, and *Muribaculaceae*. The taurocholic acid level positively correlated with the abundance of several genera including *Elusimicrobium*, *Muribaculum*, *Candidatus_Obscuribacter*, *Eubacterium*, *Parabacteroides*, and *Prevotella*, whereas negatively correlated with *Prevotella*. Taurocholic acid was shown to affect the populations of gut bacteria (Wolf et al., 2020). Ridlon et al. showed that taurocholic acid can stimulate intestinal bacteria to convert cholic acid and taurine to deoxycholic acid and hydrogen sulfide, a tumor- and genotoxin-promoter, respectively (Ridlon et al., 2016). The glutathione level positively correlated with the abundance of phylum including *Bacteroidota*. In our study, increased level of glutathione induced by PM_{2.5} was involved in thyroid hormone synthesis, which was further

found to be related to *Bacteroidota* at the phylum level. TG was found to bind to extracellular matrix and thyroid follicles in rats with PM_{2.5}-thyrotoxicity, thus strengthening the gut-thyroid relationship and the correlation with TPO level (Naiyer et al., 2008). Study showed that glutathione can improve the TPO activity, which is the enzyme involved in thyroid hormone synthesis, and can rescue metabolism from severe thyroid dysfunction (Palazzolo and Ely, 2015). The levels of kynurenic acid, a metabolite of tryptophan metabolism, positively correlated with the abundance of several phyla including *Firmicutes*, *Bacteroidota* and *Proteobacteria*. The levels of D-Glutamic acid, a metabolite of D-Glutamine and D-glutamate metabolism, positively correlated with the relative abundance of several phyla including *Proteobacteria*, *Firmicutes*, and *Bacteroidota*. The levels of citric acid, a metabolite of citrate cycle, positively correlated with the abundance of several phyla including *Firmicutes*, *Elusimicrobiota*, *Bacteroidota*, *Campilobacterota* and *Cyanobacteria*. Collectively, these results suggest that the changes in the gut microbiome were correlated with alterations in urine metabolites. The above analyses suggest that PM_{2.5} could affect the flora and its biological functions by affecting the changes of metabolites involved in the key metabolic pathways identified above, thus affecting the thyroid function. We found PM_{2.5} decreased several *Firmicutes* families, some of which are butyrate producers (Tremaroli and Backhed, 2012). Therefore, PM_{2.5}-induced gut microbiome might impact adipogenesis, short-chain fatty acid production, and energy harvesting. Moreover, fatty acid carnitines, which transport fatty acids into mitochondria for fatty acid oxidation to generate metabolic energy (Negrao et al., 1987), were observed to decrease in urine of PM_{2.5}-treated rats. This may be a compensation for energy harvest. So we concluded that the gut microbiome could regulate glucose, lipid and cholesterol metabolisms by hydrolyzing bile acid, resulting in hormonal release. These results indicate the causality between perturbation changes in microbiota induced by PM_{2.5} and thyroid function-related metabolic profile.

All in all, our study revealed PM_{2.5}-induced alteration in gut microbiome in terms of both abundance and physiology, as well as the related metabolomic profiles. The alterations in the metabolic profiles of gut microbiome might be due to regulation of bacterial gene and protein expression. A recent report showed that xenobiotics induced remarkable changes in physiology and gene expression of human gut microbiome (Maurice et al., 2013). These results indicate that a correlation might exist between gut microbiota composition disruption and diversity increase and metabolite homeostasis disorder, which ultimately promotes thyroid injury after PM_{2.5} exposure.

This study has some limitations. First, the effective components of PM_{2.5} were not investigated in detail. Second, more thorough information on correlations between gut microbiome, metabolites and biochemical parameters is required. Moreover, a better rat model with a standardized murine microbiome should be used to reduce individual variations in gut microbiota. Finally, the present study did not explore the possible difference in gut microbiome and metabolic response to PM_{2.5} exposure between males and females.

5. Conclusions

In this study, 16S rRNA gene sequencing and LC-MS based metabolomics analysis were applied to reveal the effect of PM_{2.5} exposure on rat gut microbiome and metabolic profile, and explore the potential mechanisms of thyrotoxicity. The sequencing showed that the alteration in gut microflora composition induced by PM_{2.5} exposure may be one of the pathogenic phenomena of PM_{2.5} exposure-induced thyrotoxicity. With exposure to PM_{2.5}, the altered flora can affect thyroid function, whereas a series of metabolites were substantially impacted by PM_{2.5}. In addition, some gut microbiotas were significantly correlated with the altered urine metabolites. Taken together, this study may shed new light on mechanism underlying PM_{2.5}-induced thyroid injury. Furthermore, the altered gut microflora-associated metabolites can act as biomarkers for probing the thyroid functional impacts of PM_{2.5} or other environmental chemicals.

More research is warranted to unravel the mechanisms of gut-thyroid axis interaction affected by PM_{2.5}.

Funding

This work was supported by the Natural Science Foundation of Henan Province (202300410312); the National Natural Science Foundation of China (U2004102).

CRediT authorship contribution statement

Xinwen Dong: Conceptualization, Writing – original draft, Writing – review & editing. **Sanqiao Yao:** Data curation. **Lvfei Deng:** Formal analysis, Validation. **Haibin Li:** Formal analysis. **Fengquan Zhang:** Resources, Software, Supervision, Validation. **Jie Xu:** Software, Supervision, Validation. **Zhichun Li:** Methodology. **Li Zhang:** Software, Supervision. **Jing Jiang:** Project administration. **Weidong Wu:** Writing – review & editing.

Declaration of competing interest

The authors declare that they have no competing interests.

Acknowledgments

We thank our team for their valuable assistance, and we would also like to thank Wuhan servicebio technology CO., LTD (<http://www.servicebio.cn/>) for technical support in the tissues assay and analysis of the HE and IHC data. In addition, we would also like to thank BMK Biotechnology Co., LTD (<http://www.biomarker.com.cn/>) and its technical platform BMKCloud (www.biocloud.net) for analysis support in 16S rRNA gene sequencing and LC-MS based metabolomics researches.

Appendix A. Supplementary data

Supplementary data to this article can be found online at <https://doi.org/10.1016/j.scitotenv.2022.156402>.

References

- Ahn, H.S., Kim, H.J., Kim, K.H., Lee, Y.S., Han, S.J., Kim, Y., Ko, M.J., Brito, J.P., 2016. Thyroid cancer screening in South Korea increases detection of papillary cancers with no impact on other subtypes or thyroid cancer mortality. *Thyroid* 26, 1535–1540.
- Bray, F., Ferlay, J., Soerjomataram, I., Siegel, R.L., Torre, L.A., Jemal, A., 2018. Global cancer statistics 2018: GLOBOCAN estimates of incidence and mortality worldwide for 36 cancers in 185 countries. *CA Cancer J. Clin.* 68, 394–424.
- Cai, Z., Liu, Q., 2021. Understanding the Global Cancer Statistics 2018: implications for cancer control. *Sci. China Life Sci.* 64, 1017–1020.
- Chen, D., Liu, X., Lang, J., Zhou, Y., Wei, L., Wang, X., Guo, X., 2017. Estimating the contribution of regional transport to PM_{2.5} air pollution in a rural area on the North China Plain. *Sci. Total Environ.* 583, 280–291.
- Chu, H., Huang, F.Q., Yuan, Q., Fan, Y., Xin, J., Du, M., Wang, M., Zhang, Z., Ma, G., 2021. Metabolomics identifying biomarkers of PM_{2.5} exposure for vulnerable population: based on a prospective cohort study. *Environ. Sci. Pollut. Res. Int.* 28, 14586–14596.
- Colao, A., Muscogiuri, G., Piscitelli, P., 2016. Environment and health: not only cancer. *Int. J. Environ. Res. Public Health* 13.
- Cui, J., Fu, Y., Lu, R., Bi, Y., Zhang, L., Zhang, C., Aschner, M., Li, X., Chen, R., 2019. Metabolomics analysis explores the rescue to neurobehavioral disorder induced by maternal PM_{2.5} exposure in mice. *Ecotoxicol. Environ. Saf.* 169, 687–695.
- Darbre, P.D., 2018. Overview of air pollution and endocrine disorders. *Int. J. Gen. Med.* 11, 191–207.
- DiStefano III, J.J., de Luze, A., Nguyen, T.T., 1993. Binding and degradation of 3,5,3'-triiodo-L-thyronine and thyroxine by rat intestinal bacteria. *Am. J. Phys.* 264, E966–E972.
- Dong, X., Wu, W., Yao, S., Li, H., Li, Z., Zhang, L., Jiang, J., Xu, J., Zhang, F., 2021a. PM_{2.5} disrupts thyroid hormone homeostasis through activation of the hypothalamic-pituitary-thyroid (HPT) axis and induction of hepatic transthyretin in female rats 2.5. *Ecotoxicol. Environ. Saf.* 208, 111720.
- Dong, X.W., Wu, W.D., Yao, S.Q., Zhang, Y.B., Wang, C., Wu, H.Y., Na, X.L., 2021b. Long-term di-(2-ethylhexyl) phthalate exposure disturbs the lipid metabolism profiles and hepatic enzymes in male rats: a UPLC-MS-based serum metabolomics analysis. *Biomed. Environ. Sci.* 34, 920–925.
- Fekete, C., Gereben, B., Doleschall, M., Harney, J.W., Dora, J.M., Bianco, A.C., Sarkar, S., Liposits, Z., Rand, W., Emerson, C., Kacsokovics, I., Larsen, P.R., Lechan, R.M., 2004. Lipopolysaccharide induces type 2 iodothyronine deiodinase in the mediobasal hypothalamus: implications for the nonthyroidal illness syndrome. *Endocrinology* 145, 1649–1655.
- Fernandez-Pastor, J.M., Morell, M., Menendez-Patterson, A., Escobar-Bueno, M.C., 1983. Effect of experimental changes in thyroid function on oxidative metabolism and glutamate dehydrogenase activity in the limbic system of the rat. *Rev. Esp. Fisiol.* 39, 311–316.
- Giannoula, E., Melidis, C., Frangos, S., Papadopoulos, N., Koutsouki, G., Iakovou, I., 2020. Ecological study on thyroid cancer incidence and mortality in association with European Union member States' air pollution. *Int. J. Environ. Res. Public Health* 18.
- Holmes, E., Li, J.V., Athanasiou, T., Ashrafian, H., Nicholson, J.K., 2011. Understanding the role of gut microbiome-host metabolic signal disruption in health and disease. *Trends Microbiol.* 19, 349–359.
- Howe, C.G., Eckel, S.P., Habre, R., Girguis, M.S., Gao, L., Lurmann, F.W., Gilliland, F.D., Breton, C.V., 2018. Association of prenatal exposure to ambient and traffic-related air pollution with newborn thyroid function: findings from the children's health study. *JAMA Netw. Open* 1, e182172.
- Ilias, I., Kakoulidis, I., Trogias, S., Stergiotis, S., Michou, A., Lekkou, A., Mastrodimou, V., Pappa, A., Venaki, E., Koukkou, E., 2020. Atmospheric pollution and thyroid function of pregnant women in Athens, Greece: a pilot study. *Med. Sci. (Basel)* 8.
- Irizar, A., Txintxurreta, A., Molinuevo, A., Jimeno-Romero, A., Anabitarte, A., Alvarez, J.I., Martinez, M.D., Santa-Marina, L., Ibarluzea, J., Lertxundi, A., 2021. Association between prenatal exposure to air pollutants and newborn thyroxine (T4) levels. *Environ. Res.* 111132.
- Jin, Y., Wu, Z., Wang, N., Duan, S., Wu, Y., Wang, J., Wu, W., Feng, F., 2016. Association of EGF receptor and NLRs signaling with cardiac inflammation and fibrosis in mice exposed to fine particulate matter. *J. Biochem. Mol. Toxicol.* 30, 429–437.
- Kim, H.J., Kwon, H., Yun, J.M., Cho, B., Park, J.H., 2020. Association between exposure to ambient air pollution and thyroid function in Korean adults. *J. Clin. Endocrinol. Metab.* 105.
- Kitahara, C.M., Sosa, J.A., 2016. The changing incidence of thyroid cancer. *Nat. Rev. Endocrinol.* 12, 646–653.
- Kroemer, G., Galluzzi, L., Vandenabeele, P., Abrams, J., Alnemri, E.S., Baehrecke, E.H., Blagosklonny, M.V., El-Deiry, W.S., Golstein, P., Green, D.R., Hengartner, M., Knight, R.A., Kumar, S., Lipton, S.A., Malorni, W., Nunez, G., Peter, M.E., Tschopp, J., Yuan, J., Piacentini, M., Zhivotovskiy, B., Melino, G., <collab>Nomenclature Committee on Cell, D.collab, 2009. Classification of cell death: recommendations of the Nomenclature Committee on Cell Death 2009. *Cell Death Differ.* 16, 3–11.
- Lerner, A., Jeremias, P., Matthias, T., 2017. Gut-thyroid axis and celiac disease. *Endocr. Connect.* 6, R52–R58.
- Li, A., Li, T., Gao, X., Yan, H., Chen, J., Huang, M., Wang, L., Yin, D., Li, H., Ma, R., Zeng, Q., Ding, S., 2021a. Gut microbiome alterations in patients with thyroid nodules. *Front. Cell. Infect. Microbiol.* 11, 643968.
- Li, J., Hu, Y., Liu, L., Wang, Q., Zeng, J., Chen, C., 2020. PM_{2.5} exposure perturbs lung microbiome and its metabolic profile in mice. *Sci. Total Environ.* 721, 137432.
- Li, M., Pei, J., Xu, M., Shu, T., Qin, C., Hu, M., Zhang, Y., Jiang, M., Zhu, C., 2021b. Changing incidence and projections of thyroid cancer in mainland China, 1983–2032: evidence from cancer incidence in five continents. *Cancer Causes Control* 32, 1095–1105.
- Lin, X., Zhao, J., Zhang, W., He, L., Wang, L., Li, H., Liu, Q., Cui, L., Gao, Y., Chen, C., Li, B., Li, Y.F., 2021. Towards screening the neurotoxicity of chemicals through feces after exposure to methylmercury or inorganic mercury in rats: a combined study using gut microbiome, metabolomics and metalomics. *J. Hazard. Mater.* 409, 124923.
- Lui, K.H., Jones, T., Berube, K., Ho, S.S.H., Yim, S.H.L., Cao, J.J., Lee, S.C., Tian, L., Min, D.W., Ho, K.F., 2019. The effects of particle-induced oxidative damage from exposure to airborne fine particulate matter components in the vicinity of landfill sites on Hong Kong. *Chemosphere* 230, 578–586.
- Maurice, C.F., Haiser, H.J., Turnbaugh, P.J., 2013. Xenobiotics shape the physiology and gene expression of the active human gut microbiome. *Cell* 152, 39–50.
- Moshkelgosha, S., Masetti, G., Berchner-Pfannschmidt, U., Verhasselt, H.L., Horstmann, M., Diaz-Cano, S., Noble, A., Edelman, B., Covelli, D., Plummer, S., Marchesi, J.R., Ludgate, M., Biscarini, F., Eckstein, A., Banga, J.P., 2018. Gut microbiome in BALB/c and C57BL/6J mice undergoing experimental thyroid autoimmunity associate with differences in immunological responses and thyroid function. *Horm. Metab. Res.* 50, 932–941.
- Nadolnik, L.I., Niatsetskaia, Z.V., Lupachyk, S.V., 2008. Effect of oxidative stress on rat thyrocyte iodide metabolism. *Cell Biochem. Funct.* 26, 366–373.
- Naiyer, A.J., Shah, J., Hernandez, L., Kim, S.Y., Ciaccio, E.J., Cheng, J., Manavalan, S., Bhagat, G., Green, P.H., 2008. Tissue transglutaminase antibodies in individuals with celiac disease bind to thyroid follicles and extracellular matrix and may contribute to thyroid dysfunction. *Thyroid* 18, 1171–1178.
- Negrao, C.E., Ji, L.L., Schauer, J.E., Nagle, F.J., Lardy, H.A., 1987. Carnitine supplementation and depletion: tissue carnitines and enzymes in fatty acid oxidation. *J. Appl. Physiol.* 63, 315–321.
- Neven, K.Y., Wang, C., Janssen, B.G., Roels, H.A., Vanpoucke, C., Ruttens, A., Nawrot, T.S., 2021. Ambient air pollution exposure during the late gestational period is linked with lower placental iodine load in a Belgian birth cohort. *Environ. Int.* 147, 106334.
- Palazzolo, D.L., Ely, E.A., 2015. Arsenic trioxide and reduced glutathione act synergistically to augment inhibition of thyroid peroxidase activity in vitro. *Biol. Trace Elem. Res.* 165, 110–117.
- Pan, S., Ni, W., Li, W., Li, G., Xing, Q., 2019. Effects of PM_{2.5} and PM₁₀ on congenital hypothyroidism in Qingdao, China, 2014–2017: a quantitative analysis. *Ther. Adv. Endocrinol. Metab.* 10 2042018819892151.
- Ren, B., Wan, S., Liu, L., Qu, M., Wu, H., Shen, H., 2021. Distributions of serum thyroid-stimulating hormone in 2020 thyroid disease-free adults from areas with different iodine levels: a cross-sectional survey in China. *J. Endocrinol. Investig.* 44, 1001–1010.
- Ridlon, J.M., Wolf, P.G., Gaskins, H.R., 2016. Tauracholic acid metabolism by gut microbes and colon cancer. *Gut Microbes* 7, 201–215.
- Riggs, D.W., Zafar, N., Krishnasamy, S., Yeager, R., Rai, S.N., Bhatnagar, A., O'Toole, T.E., 2020. Exposure to airborne fine particulate matter is associated with impaired

- endothelial function and biomarkers of oxidative stress and inflammation. *Environ. Res.* 180, 108890.
- Robitaille, R., 1995. Purinergic receptors and their activation by endogenous purines at perisynaptic glial cells of the frog neuromuscular junction. *J. Neurosci.* 15, 7121–7131.
- Shang, L., Huang, L., Yang, W., Qi, C., Yang, L., Xin, J., Wang, S., Li, D., Wang, B., Zeng, L., Chung, M.C., 2019. Maternal exposure to PM2.5 may increase the risk of congenital hypothyroidism in the offspring: a national database based study in China. *BMC Public Health* 19, 1412.
- Su, X., Zhao, Y., Li, Y., Ma, S., Wang, Z., 2020. Gut dysbiosis is associated with primary hypothyroidism with interaction on gut-thyroid axis. *Clin. Sci. (Lond.)* 134, 1521–1535.
- Tremaroli, V., Backhed, F., 2012. Functional interactions between the gut microbiota and host metabolism. *Nature* 489, 242–249.
- van der Boom, T., Gruppen, E.G., Lefrandt, J.D., Connelly, M.A., Links, T.P., Dullaart, R.P.F., 2020. Plasma branched chain amino acids are lower in short-term profound hypothyroidism and increase in response to thyroid hormone supplementation. *Scand. J. Clin. Lab. Invest.* 80, 562–566.
- Villanger, G.D., Drover, S.S.M., Nethery, R.C., Thomsen, C., Sakhi, A.K., Overgaard, K.R., Zeiner, P., Hoppin, J.A., Reichborn-Kjennerud, T., Aase, H., Engel, S.M., 2020. Associations between urine phthalate metabolites and thyroid function in pregnant women and the influence of iodine status. *Environ. Int.* 137, 105509.
- Virili, C., Stramazzo, I., Centanni, M., 2021. Gut microbiome and thyroid autoimmunity. *Best Pract. Res. Clin. Endocrinol. Metab.* 35, 101506.
- Wahlang, B., Alexander II, N.C., Li, X., Rouchka, E.C., Kirpich, I.A., Cave, M.C., 2021. Polychlorinated biphenyls altered gut microbiome in CAR and PXR knockout mice exhibiting toxicant-associated steatohepatitis. *Toxicol. Rep.* 8, 536–547.
- Wang, H., Song, L., Ju, W., Wang, X., Dong, L., Zhang, Y., Ya, P., Yang, C., Li, F., 2017. The acute airway inflammation induced by PM2.5 exposure and the treatment of essential oils in Balb/c mice. *Sci. Rep.* 7, 44256.
- Wang, H.T., Liang, Z.Z., Ding, J., Xue, X.M., Li, G., Fu, S.L., Zhu, D., 2021. Arsenic bioaccumulation in the soil fauna alters its gut microbiome and microbial arsenic biotransformation capacity. *J. Hazard. Mater.* 417, 126018.
- Wang, L.L., Li, H.Q., Chang, Q.G., Li, S., Yin, D.T., 2020. Clinical pathology and incidence trend of thyroid cancer based on 21 980 cases. *Zhonghua Yi Xue Za Zhi* 100, 1072–1076.
- Wang, X., Liu, C., Zhang, M., Han, Y., Aase, H., Villanger, G.D., Myhre, O., Donkelaar, A.V., Martin, R.V., Baines, E.A., Chen, R., Kan, H., Xia, Y., 2019. Evaluation of maternal exposure to PM2.5 and its components on maternal and neonatal thyroid function and birth weight: a cohort study. *Thyroid* 29, 1147–1157.
- White, J.R., Nagarajan, N., Pop, M., 2009. Statistical methods for detecting differentially abundant features in clinical metagenomic samples. *PLoS Comput. Biol.* 5, e1000352.
- Wirth, S., Syleouni, M.E., Karavasiloglou, N., Rinaldi, S., Korol, D., Wanner, M., Rohrmann, S., 2021. Incidence and mortality trends of thyroid cancer from 1980 to 2016. *Swiss Med. Wkly.* 151, w30029.
- Wolf, P.G., Gaskins, H.R., Ridlon, J.M., Freels, S., Hamm, A., Goldberg, S., Pettrilli, P., Schering, T., Vergis, S., Gomez-Perez, S., Yazici, C., Braunschweig, C., Mutlu, E., Tussing-Humphreys, L., 2020. Effects of taurocholic acid metabolism by gut bacteria: a controlled feeding trial in adult African American subjects at elevated risk for colorectal cancer. *Contemp. Clin. Trials Commun.* 19, 100611.
- Wu, W., Sun, Y., Luo, N., Cheng, C., Jiang, C., Yu, Q., Cheng, S., Ge, J., 2021. Integrated 16S rRNA gene sequencing and LC-MS analysis revealed the interplay between gut microbiota and plasma metabolites in rats with ischemic stroke. *J. Mol. Neurosci.* 71, 2095–2106.
- Xu, M.X., Zhu, Y.F., Chang, H.F., Liang, Y., 2016. Nanoceria restrains PM2.5-induced metabolic disorder and hypothalamus inflammation by inhibition of astrocytes activation related NF-kappaB pathway in Nrf2 deficient mice. *Free Radic. Biol. Med.* 99, 259–272.
- Xu, Y., Wang, W., Zhou, J., Chen, M., Huang, X., Zhu, Y., Xie, X., Li, W., Zhang, Y., Kan, H., Ying, Z., 2019. Metabolomics analysis of a mouse model for chronic exposure to ambient PM2.5. *Environ. Pollut.* 247, 953–963.
- Zeng, Y., He, H., Wang, X., Zhang, M., An, Z., 2020. Climate and air pollution exposure are associated with thyroid function parameters: a retrospective cross-sectional study. *J. Endocrinol. Investig.* 44, 1515–1523.
- Zhang, J., Zhang, F., Zhao, C., Xu, Q., Liang, C., Yang, Y., Wang, H., Shang, Y., Wang, Y., Mu, X., Zhu, D., Zhang, C., Yang, J., Yao, M., Zhang, L., 2019. Dysbiosis of the gut microbiome is associated with thyroid cancer and thyroid nodules and correlated with clinical index of thyroid function. *Endocrine* 64, 564–574.
- Zhang, Y., Hu, H., Shi, Y., Yang, X., Cao, L., Wu, J., Asweto, C.O., Feng, L., Duan, J., Sun, Z., 2017. (1)H NMR-based metabolomics study on repeat dose toxicity of fine particulate matter in rats after intratracheal instillation. *Sci. Total Environ.* 589, 212–221.
- Zhao, P., Lu, W., Hong, Y., Chen, J., Dong, S., Huang, Q., 2021. Long-term wet precipitation of PM2.5 disturbed the gut microbiome and inhibited the growth of marine medaka *Oryzias melastigma*. *Sci. Total Environ.* 755, 142512.
- Zhao, Y., Cao, Z., Li, H., Su, X., Yang, Y., Liu, C., Hua, J., 2019. Air pollution exposure in association with maternal thyroid function during early pregnancy. *J. Hazard. Mater.* 367, 188–193.